NJC

Methane Conversion on Cobalt-Added Liquid-Metal Indium Catalysts

Journal:	*New Journal of Chemistry*
Manuscript ID	NJ-LET-07-2020-003808.R1
Article Type:	Letter
Date Submitted by the Author:	02-Sep-2020
Complete List of Authors:	Tajima, Hiroki; Saitama University Ogihara, Hitoshi; Saitama University, Yoshida-Hirahara, Miru; Sophia University, Department of Materials and Life Sciences; Saitama University, Research and Development Bureau Kurokawa, Hideki; Saitama University, Graduate School of Science & Engineering

COMMUNICATION

Methane Conversion on Cobalt-Added Liquid-Metal Indium Catalysts

Hiroki Tajima,[a] Hitoshi Ogihara,[a] Miru Yoshida-Hirahara[a] Hideki Kurokawa[a]*

Received 00th January 20xx,
Accepted 00th January 20xx

DOI: 10.1039/x0xx00000x

Non-oxidative methane (CH_4) conversion was carried out using a silica-supported cobalt-added indium liquid metal catalyst (In-Co/SiO_2). In-Co/SiO_2 showed different activity from In/SiO_2 and Co/SiO_2. In-Co/SiO_2 promoted the formation of aromatics (e.g., benzene) from CH_4. The ethylene conversion reaction implied that Co present in indium liquid metal was effective for the aromatization reaction. We propose bifunctional catalysis by In-Co for CH_4 conversion: (1) indium liquid metal activates CH_4 molecules to form C_2 hydrocarbons by CH_4 coupling, and (2) a portion of C_2 hydrocarbons is converted to aromatics by Co species present in the liquid metal. This work was compared to reported systems such as supported catalytically active liquid metal solutions (SCALMS).

Petroleum is a raw material in the production of basic chemicals, such as olefins and aromatic compounds, but faces a depletion problem in the future. Therefore, natural gas is expected to be used for the production of essential chemicals, and recent development of the shale gas extraction technology also boosts the use of natural gas in chemical industries. However, methane (CH_4), the main component of natural gas, is difficult to convert to useful chemicals because of its high stability that is attributed to strong C-H bonds and a symmetrical molecular structure [1]. For several decades, chemical conversion of CH_4 has been intensely investigated [2-5], and a dehydrogenative route is one of the most promising processes for CH_4 conversion [6-13]. In the dehydrogenative process, CH_4 is converted into hydrogen, C_2 hydrocarbons, and aromatics. However, catalyst deactivation due to coke deposition is a crucial problem. Therefore, the design of catalysts with high coking resistance is necessary. So far, various catalysts have been reported, and liquid metal (LM) is currently being paid attention to as a new catalyst for CH_4 conversion. Molten metal catalysts that can diminish the deactivation by coke deposition have been examined in the complete dehydrogenation of CH_4 to form hydrogen and separable carbon [14]. Recently, it is reported that low melting-point metals, such as indium (In) and bismuth (Bi), are effective for dehydrogenative CH_4 conversion, where In and Bi LMs catalyze CH_4 activation, and C_2 hydrocarbons and aromatics are produced [7, 15, 16].

On the other hand, Wasserscheid and coworkers recently developed the idea of supported catalytically active liquid metal solutions (SCALMS); SCALMS presumably have homogeneously distributed metal atoms at the surface of a liquid metallic phase [17-19]. For example, a liquid mixture of Ga (melting point is 303 K) and Pd deposited on porous glass was active for butane dehydrogenation, and was insensitive to deactivation by coke deposition [17]. In addition, for propane dehydrogenation in the presence of CO, $Ga_{37}Pt/Al_2O_3$ SCALMS showed higher conversion than Pt/Al_2O_3 because of its high tolerance to the poisoning effect of CO adsorption and coke [18]. These studies also suggested that the noble metals (Pd or Pt) added to Ga are present as isolated noble-metal atoms at the surface of a liquid Ga matrix, where it is considered that Ga LM is inert for catalytic reactions, and the isolated noble-metal atoms act as unique catalysts. Furthermore, it is reported that liquid metal galinstan containing Rh catalysts is effective for hydroformylation of olefins [20].

As described above, researches on catalysis by LM are categorized into two concepts: (1) the catalysis by LMs themselves (e.g. molten metals and low melting point metals) and (2) the catalysis by isolated metal atoms on SCALMS. In this study, CH_4 conversion was performed on an In-Co catalyst in which Co was added as a second component to In LM. In-Co acted as a bi-functional catalyst to convert CH_4 into value-added molecules: In LM converted CH_4 into C_2 hydrocarbons, and successively the added Co species promoted the aromatization of the formed C_2 hydrocarbons. The synergy effect of LM and the secondary component (Co) has been considered, and it may help shed light on catalysis in hydrocarbon conversion processes.

[a] *Graduate School of Science and Engineering, Saitama University, 255 Shimo-Okubo, Sakura-ku, Saitama 338-8570, Japan*

† Footnotes relating to the title and/or authors should appear here.
Electronic Supplementary Information (ESI) available: [details of any supplementary information available should be included here]. See DOI: 10.1039/x0xx00000x

Table 1 Reaction results of CH_4 conversion at 1073 K. Catalyst mass: 0.2 g; flow rate: 10 mL min^{-1}; p(CH_4): 1 bar; reaction time: 2 h.

entry	catalysts	yield / μmol h^{-1} g_{cat}^{-1}								coke / mg h^{-1} g_{cat}^{-1}	conv. / %	carbon balance / %
		H_2	C_2H_6	C_2H_4	C_2H_2	C_3H_6	C_6H_6	C_7H_8	$C_{10}H_8$			
1	SiO_2	200	19.1	8	n.d.	1	n.d.	n.d.	n.d.	1	0.1	98.5
2	Co/SiO_2	665	51.1	60	2.0	6	n.d.	n.d.	n.d.	3	0.4	99.3
3	In/SiO_2	3025	74.7	207	6.0	13	n.d.	n.d.	n.d.	15	1.6	100.8
4	In-Co (1) $/SiO_2$	4250	55.3	248	6.1	19	1.4	n.d.	n.d.	22	2.1	99.5
5	In-Co (2) $/SiO_2$	4486	53.3	261	5.9	21	2.7	0.7	0.5	23	2.2	97.7
6	In-Co (9) $/SiO_2$	5281	49.1	262	4.8	22	4.0	1.2	0.6	28	2.6	99.1
7	In-Co (17) $/SiO_2$	5648	47.5	253	4.1	20	4.9	1.4	0.6	30	2.7	99.6
8	In-Co (50) $/SiO_2$	5874	42.5	229	3.7	19	5.3	1.4	0.7	32	2.8	100.0

All catalysts were prepared by a typical impregnation method. Loading of In was 5 wt% in all catalysts. The loading of Co in Co/SiO_2 was 0.5 wt%. In-Co/SiO_2 catalysts with 1, 2, 9, 17, 50 atomic% of Co were prepared, and hereafter denoted as In-Co(1), In-Co(2), In-Co(9), In-Co(17), and In-Co(50)/SiO_2, respectively. The Co loadings for In-Co(1), In-Co(2), In-Co(9), In-Co(17), and In-Co(50)/SiO_2 were 0.026, 0.051, 0.26, 0.51, and 2.6 wt%, respectively. The detail in CH_4 and ethylene (C_2H_4) conversion reactions, a schematic of reaction system (Fig. S1) and catalyst characterization are shown in supplementary data.

Table 1 summarizes the reaction results for dehydrogenative conversion of CH_4 on various catalysts. Products for CH_4 conversion were C_2 hydrocarbons (C_2H_6, C_2H_4, and C_2H_2), propylene (C_3H_6), aromatics (C_6H_6, C_7H_8, and $C_{10}H_8$), and coke. For all catalysts, except for SiO_2, the main hydrocarbon product was C_2H_4. Time courses for CH_4 conversion and formation rate for gaseous products are shown in Fig. S2. When using only SiO_2 (entry 1), CH_4 hardly converted, which indicated CH_4 is so stable that pyrolysis did not proceed at 1073 K. As previously reported, In/SiO_2 was active for the reaction [7]; the yield of C_2H_4 was much higher than SiO_2 (entries 1 and 3). For Co/SiO_2 (entry 2), the reaction proceeded, but the amount of formed hydrocarbon was inferior to In/SiO_2. For In-Co/SiO_2, the yields of the main product (C_2H_4) were higher than In/SiO_2 and Co/SiO_2, regardless of the In-Co ratio. Interestingly, the formation of aromatics (i.e., benzene, toluene, and naphthalene) was observed with In-Co/SiO_2, while aromatics were not detected for In/SiO_2 and Co/SiO_2. The results suggest that In-Co/SiO_2 has different catalytic functions than In/SiO_2 and Co/SiO_2; In-Co/SiO_2 had higher activities for CH_4 coupling and aromatization reactions than In/SiO_2 and Co/SiO_2. TG/DTA analysis for In-Co(17)/SiO_2 after reaction was carried out, and we can see that the weight loss for coke combustion was 3~4 wt% (Fig. S3).

Table 2 shows product yields for the conversion of C_2H_4 in the presence of H_2 at 1023 K on In-Co(17)/SiO_2, In/SiO_2, Co/SiO_2, and SiO_2. Note that the reaction temperature for C_2H_4 was lower than CH_4 conversion (Table 1) and H_2 was coexisted in C_2H_4 because C_2H_4 has higher reactivity than CH_4. Time courses for C_2H_4 conversion and formation rate for gaseous products are shown in Fig. S4. In the reactions, CH_4 (a cracking product), C_2H_6 (a hydrogenation product), trace amounts of C_3 hydrocarbons, aromatics, and coke were formed. For SiO_2 and In/SiO_2 (entries 9 and 11), similar reaction results were observed, which indicated that In LM has no catalytic activity for converting C_2H_4. Compared to In/SiO_2, Co/SiO_2 promoted the formation of CH_4, C_2H_6, C_2H_2, and aromatics (entry 10). Interestingly,

Table 2 Reaction results of C_2H_4 conversion at 1023 K. Catalyst mass: 0.5 g; flow rate of mixture of Ar/H_2/C_2H_4: 47/3/3 mL min^{-1}; reaction time: 2 h.

entry	catalysts	yield / μmol h^{-1} g_{cat}^{-1}							coke / mg h^{-1} g_{cat}^{-1}	conv. / %	carbon balance / %
		CH_4	C_2H_6	C_2H_2	C_3H_6	C_6H_6	C_8H_8	$C_{10}H_8$			
9	SiO_2	91	243	133	26	0.9	n.d.	n.d.	3	3.8	95.6
10	Co/SiO_2	114	290	228	29	4.5	n.d.	0.3	9	6.6	97.5
11	In/SiO_2	26	185	183	5	n.d.	n.d.	n.d.	3	3.1	92.7
12	In-Co(17)/SiO_2	572	340	86	31	15.9	0.6	1.5	31	13.4	91.4

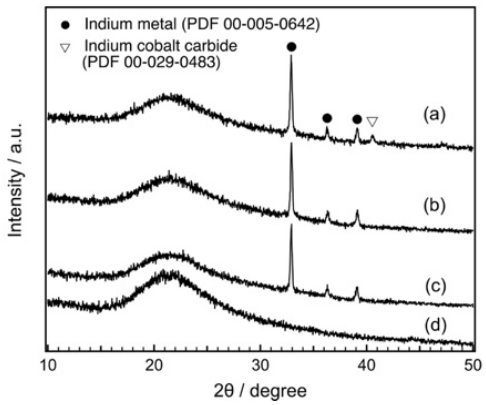

Fig. 1. XRD patterns of (a) In-Co(17)/SiO_2 after CH_4 conversion reaction, (b) In/SiO_2 after CH_4 conversion reaction, (c) In/SiO_2 after reduction with H_2, and (d) Co/SiO_2 after CH_4 conversion reaction.

In-Co(17)/SiO_2 (entry 12) showed higher yields of CH_4, C_2H_6 and aromatics than Co/SiO_2 and In/SiO_2. Here, it should be noted that In-Co(17)/SiO_2 showed the highest aromatics yields for C_2H_4 conversion in Table 2. The results shown in Table 2 indicated that the aromatization is strongly promoted on Co interacted with In LM.

In/SiO_2 is reported as an effective catalyst for dehydrogenative coupling of CH_4 to form C_2 hydrocarbons [7]. The structure of In catalysts was examined using temperature programmed XRD [7], first-principle molecular dynamics calculation [15], and in-situ X-ray absorption fine structure analysis [16], revealing that In is present as LM and the liquid-state is the origin for the catalysis of CH_4 coupling. In this study, we used Co added In/SiO_2, and according to the phase diagram of In-Co [21], a few percent of Co dissolves in In LM at reaction temperature (1073 K). Therefore, it is considered that a part of added Co dissolved in In LM particles under reaction condition and it is likely that the dissolved Co showed different catalytic activity from Co supported on SiO_2. However, the LM state of In and the dissolution of Co in LM In at reaction conditions were not directly observed in this work and assumed based on the previous works [7, 15, 16].

In this regard, the effect of Co content in In-Co/SiO_2 was investigated. The results were shown in Table 1 (entries 3~8). As the Co ratio increased from 0 to 17 at%, the yields of aromatics increased, indicating Co species played a role in the aromatization. The formation of aromatics seemed to occur equally at 17 and 50 at% of Co (entries 7, 8). As mentioned above, Co dissolves in In LM at reaction temperature and the amount of dissolved Co is a few percent. We will discuss the catalysis by the dissolved Co later in detail; briefly, we consider that the dissolved Co promoted the aromatization reaction. The dissolved Co species increased with the amount of added Co, which would promote the formation of aromatics. It is considered that not all of the added Co necessarily dissolved in the In particles, so that a part of Co was supported on the SiO_2 support apart from In LM. Therefore, when Co exceeding the solubility limitation was added, the dissolution of Co in In LM reached the limitation. Considering the result that the aromatics yields were

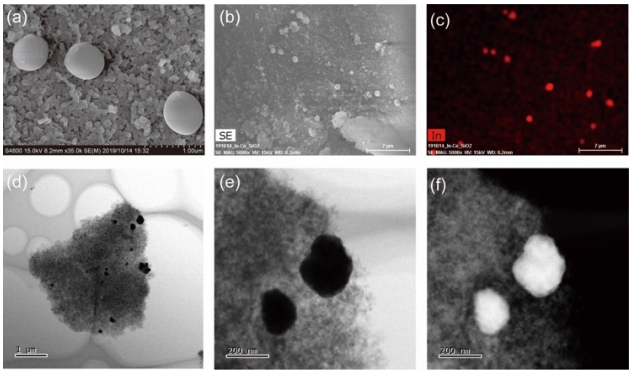

Fig. 2. (a, b) SEM, (c) EDX mapping of In, (d, e) TEM, and (f) STEM images for In-Co(17)/SiO_2 after CH_4 conversion reaction.

almost the same for 17 and 50 at% of Co, we assume that the addition of 17 at% of Co maximized the dissolution of Co in In LM and leveled off the aromatics formation.

Fig. 1 shows the XRD patterns of catalysts. For In/SiO_2, diffraction lines attributed to In metal were observed in before and after reactions. For In-Co(17)/SiO_2, similar XRD patterns to In/SiO_2 were observed. The phase diagram indicates that In-Co solid solution was not formed at low temperature [21], therefore, phase separation cannot be avoided at room temperature. This is because the XRD patterns of In/SiO_2 and In-Co(17)/SiO_2 were the same. For Co/SiO_2, no diffraction lines were detected because the loading of Co was quite small (0.5 wt%).

The specific surface areas of catalysts were as follows: SiO_2 (186 m^2g^{-1}), In/SiO_2 (171 m^2g^{-1}), Co/SiO_2 (163 m^2g^{-1}), and In-Co(17)/SiO_2 (173 m^2g^{-1}). Fig. 2a shows a SEM image of In-Co(17)/SiO_2 after the CH_4 dehydrogenation reaction. Spherical particles with a diameter of approx. 0.5 μm were observed. EDX analysis confirmed that the spherical particles consisted of In (Fig. 2b and 2c). The SEM and EDX analysis suggested that In was present as spherical LM under the reaction conditions. At the same time, EDX analysis for Co was performed, but information on the In-Co solid solution was not obtained, because the low loading of Co in the catalysts (e.g. 0.51 wt% for In-Co (17)/SiO_2) made it difficult to confirm Co species using EDX analysis. TEM images also indicated that large particles are present on SiO_2 support and an STEM image suggested the particles are metal (Fig. 2d-f). Temperature programmed reduction (TPR) profiles for In/SiO_2, Co/SiO_2, and In-Co(17)/SiO_2 after calcination at 1073 K are shown in Fig. S5. For In-Co(17)/SiO_2, two reduction peaks were observed at 700 and 920 K. Taking account of TPR profile of Co/SiO_2 (reduction was observed at 600~800 K) into account, the first peak would be the reduction of cobalt oxide. In addition, similar reduction peaks were observed for In-Co(17)/SiO_2 and In/SiO_2, indicating the reduction of In_2O_3. The reduction peak for In-Co(17)/SiO_2 was slightly shifted to higher temperature than In/SiO_2. The difference in reduction behaviour implies the interaction between In and Co.

Based on the above results, the reaction route of CH_4 conversion over In-Co/SiO_2 and roles of the catalysts were proposed as shown in Scheme 1. We considered that CH_4 dehydrogenation proceeds by sequential reactions. At first, a CH_4 molecule is activated by abstracting a hydrogen atom and the CH_3 species couple to form C_2H_6 (step (a) in Scheme 1). For step (a), the activation mechanism of CH_4 by In LM was proposed on the basis of density functional theory calcinations, indicating low-coordinated In atoms continuously appear on In LM surface, and promote the dissociation of C-H bond in CH_4 molecule [15]. Furthermore, it is reported that In LM works as a catalyst for C_2 hydrocarbons formation from CH_4 [7]. Indeed, the results in Table 1 suggested that In/SiO_2 showed higher CH_4 coupling activity than Co/SiO_2 and SiO_2. In-Co/SiO_2 produced almost the same amount of C_2 hydrocarbons as In/SiO_2, indicating that In LM of In-Co/SiO_2 also acted as a coupling catalyst.

$$CH_4 \xrightarrow[LM]{(a)} C_2H_6 \xrightarrow[\Delta]{(b)} C_2H_4 \xrightarrow[\substack{Co\\ in\ LM}]{(c)} \text{aromatics}$$

Scheme 1. The proposed reaction route for dehydrogenative conversion of CH_4 on In-Co/SiO_2 catalyst.

Because C_2H_6 readily converts to C_2H_4 in gas phase without catalysts at 1073 K (step (b) in Scheme 1) [22], the formation of C_2H_4 mainly occurred without the aid of catalysts. In Table 1, In-Co/SiO_2 showed slightly higher C_2H_4 yield than In/SiO_2, implying a part of C_2H_4 was produced via the dehydrogenation of C_2H_6 on Co present in LM. The final step is the aromatization of C_2 hydrocarbons. It should be noted again that C_2 hydrocarbons yields in CH_4 conversion were similar with In/SiO_2 and In-Co/SiO_2, but aromatics were observed only for In-Co/SiO_2 (Table 1). In addition, as shown in Table 2, In-Co/SiO_2 had higher catalytic activity for aromatization of C_2H_4 than In/SiO_2 and Co/SiO_2. Taking these reaction results into account, we considered that C_2H_4 formed via the coupling of CH_4 converted to aromatics by the In-Co catalyst. We presumed that Co dissolved in LM showed catalytic activity for the aromatization reaction. Although the origin of catalysis due to Co present in LM is not clear at the present, it is reported that the recombination of propargyl radicals (C_3H_3·) provides benzene during CH_4 pyrolysis [23, 24], therefore, Co in LM might promote the formation of propargyl radicals from C_2H_4.

Previous reports of LM catalysts were focused on the concept of catalysis by LM itself. Furthermore, for SCALMS system, isolated metal atoms on LM are the catalysts, where LM itself does not work as catalysts. This study is different from the previous works. We proposed a new bifunctional catalyst based on the LM system: In LM activated CH_4 molecules along with additional Co present in LM was effective for the aromatization of C_2 hydrocarbons. For In-Co/SiO_2, both LM and the added metal acted as catalysts.

Conclusions

For the dehydrogenative conversion of CH_4, In-Co/SiO_2 showed different activity from In/SiO_2 and Co/SiO_2. As previously reported, In/SiO_2 catalyzed the coupling of CH_4 to form C_2 hydrocarbons. For In-Co/SiO_2, not only the coupling activity of CH_4, but also the aromatization ability was exhibited. Examining the catalytic activity for C_2H_4, which is the main product of CH_4 conversion, it was revealed that In/SiO_2 has no activity for C_2H_4, while In-Co/SiO_2 catalyzed the aromatization of C_2H_4. SEM and EDX analysis implied that LM was present in In-Co/SiO_2. Based on the results, we propose a unique catalytic mechanism of In-Co/SiO_2 for the conversion of CH_4: LM assists CH_4 coupling and Co present in LM promotes the aromatization. Such bifunctional mechanism is proposed for the first time in an LM catalyst system.

Acknowledgement

This work is supported by the technology development project carried out in Japan Petroleum Energy Center (JPEC) under the commission of the Ministry of Economy, Trade and Industry (METI) and also by JST CREST, Grant Number JPMJCR15P4. We appreciate the technical support of Comprehensive Analysis Center for Science (Saitama University) for FE-SEM, EDX, and XRD analyses. We thank the technical support of Mr. Usui for nitrogen adsorption measurements of catalysts. A part of this work was supported by NIMS microstructural characterization platform as a program of "Nanotechnology Platform" of the Ministry of Education, Culture, Sports, Science and Technology (MEXT), Japan.

Conflicts of interest

There are no conflicts to declare.

Notes and references

1. U. P. M. Ashik, W. M. A. W. Daud and H. F. Abbas, *Renew. Sust. Energ. Rev.*, 2015, **44**, 221-256.
2. G. E. Keller and M. M. Bhasin, *J. Catal.*, 1982, **73**, 9-19.
3. K. Otsuka, K. Jinno and A. Morikawa, *Chem. Lett.*, 1985, 499-500.
4. T. Ito and J. H. Lunsford, *Nature*, 1985, **314**, 721-722.
5. L. S. Wang, L. X. Tao, M. S. Xie, G. F. Xu, J. S. Huang and Y. D. Xu, *Catal. Lett.*, 1993, **21**, 35-41.
6. X. G. Guo, G. Z. Fang, G. Li, H. Ma, H. J. Fan, L. Yu, C. Ma, X. Wu, D. H. Deng, M. M. Wei, D. L. Tan, R. Si, S. Zhang, J. Q. Li, L. T. Sun, Z. C. Tang, X. L. Pan and X. H. Bao, *Science*, 2014, **344**, 616-619.
7. Y. Nishikawa, H. Ogihara and I. Yamanaka, *ChemistrySelect*, 2017, **2**, 4572-4576.
8. J. Hu, S. J. Wu, Y. Y. Ma, X. Y. Yang, Z. F. Li, H. Liu, Q. S. Huo, J. Q. Guan and Q. B. Kan, *New J. Chem.*, 2015, **39**, 5459-5469.
9. J. Q. Hao, P. Schwach, G. Z. Fang, X. G. Guo, H. L. Zhang, H. Shen, X. Huang, D. Eggart, X. L. Pan and X. H. Bao, *ACS Catal.*, 2019, **9**, 9045-9050.
10. Y. Xiao and A. Varma, *ACS Catal.*, 2018, **8**, 2735-2740.
11. P. F. Xie, T. C. Pu, A. M. Nie, S. Hwang, S. C. Purdy, W. J. Yu,

D. Su, J. T. Miller and C. Wang, *ACS Catal.*, 2018, **8**, 4044-4048.
12. D. Gerceker, A. H. Motagamwala, K. R. Rivera-Dones, J. B. Miller, G. W. Huber, M. Mavrikakis and J. A. Dumesic, *ACS Catal.*, 2017, **7**, 2088-2100.
13. K. K. Zhao, L. T. Jia, J. G. Wang, B. Hou and D. B. Li, *New J. Chem.*, 2019, **43**, 4130-4136.
14. D. C. Upham, V. Agarwal, A. Khechfe, Z. R. Snodgrass, M. J. Gordon, H. Metiu and E. W. McFarland, *Science*, 2017, **358**, 917-920.
15. Y. Ohtsuka, Y. Nishikawa, H. Ogihara, I. Yamanaka, M. Ratanasak, A. Nakayama and J. Hasegawa, *J. Phys. Chem. A*, 2019, **123**, 8907-8912.
16. U. Kashaboina, Y. Nishikawa, Y. Wakisaka, N. Sirisit, S. Nagamatsu, D. L. Bao, H. Ariga-Miwa, S. Takakusagi, Y. Inami, F. Kuriyama, A. L. Dipu, H. Ogihara, S. Iguchi, I. Yamanaka, T. Wada and K. Asakura, *Chem. Lett.*, 2019, **48**, 1145-1147.
17. N. Taccardi, M. Grabau, J. Debuschewitz, M. Distaso, M. Brandl, R. Hock, F. Maier, C. Papp, J. Erhard, C. Neiss, W. Peukert, A. Gorling, H. P. Steinruck and P. Wasserscheid, *Nat. Chem.*, 2017, **9**, 862-867.
18. T. Bauer, S. Maisel, D. Blaumeiser, J. Vecchietti, N. Taccardi, P. Wasserscheid, A. Bonivardi, A. Gorling and J. Libuda, *ACS Catal.*, 2019, **9**, 2842-2853.
19. M. Kettner, S. Maisel, C. Stumm, M. Schwarz, C. Schuschke, A. Gorling and J. Libuda, *J. Catal.*, 2019, **369**, 33-46.
20. H. Sun, W. Guo, J. Liu, Z. Feng, R. Li, X. Zhou and J. S. Huang, *Appl. Organomet. Chem.*, 2018, **32**, e4555.
21. H. Okamoto, *J. Phase Equilib.*, 1997, **18**, 315-315.
22. H. Ogihara, H. Tajima and H. Kurokawa, *React. Chem. Eng.*, 2020, **5**, 145-153.
23. C. Keramiotis, G. Vourliotakis, G. Skevis, M. A. Founti, C. Esarte, N. E. Sanchez, A. Millera, R. Bilbao and M. U. Alzueta, *Energy*, 2012, **43**, 103-110.
24. J. A. Miller and S. J. Klippenstein, *J. Phys. Chem. A*, 2003, **107**, 7783-7799.

A text for a table of contents entry

In-Co converts CH_4 molecules by catalyzing CH_4 coupling over indium liquid metal and aromatization over Co in liquid metal.

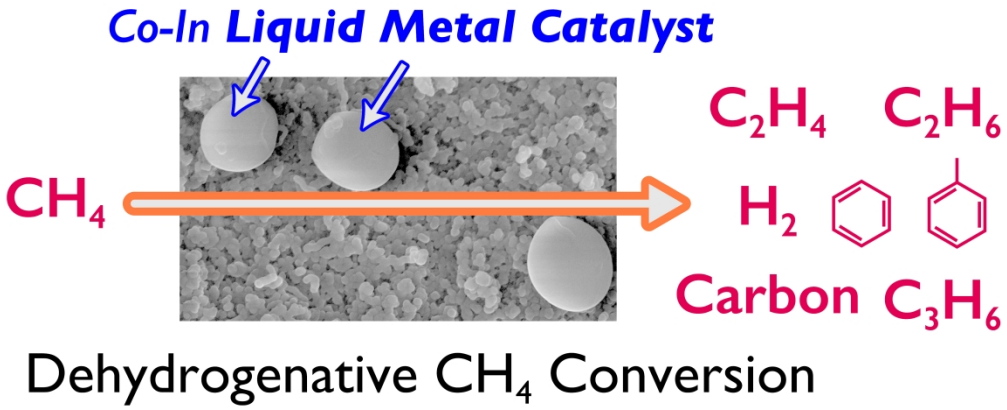

Dehydrogenative CH_4 Conversion

446x184mm (300 x 300 DPI)